

Large- N_c masses of light mesons from QCD sum rules for non-linear radial Regge trajectories

S. S. Afonin and T. D. Solomko

Saint Petersburg State University, 7/9 Universitetskaya nab., St.Petersburg, 199034, Russia

Abstract

The large- N_c masses of light vector, axial, scalar and pseudoscalar mesons are calculated from QCD spectral sum rules for a particular ansatz interpolating the radial Regge trajectories. The ansatz includes a linear part plus exponentially decreasing corrections to the meson masses and residues. The form of corrections was proposed some time ago from consistency with analytical structure of Operator Product Expansion of the two-point correlation functions. Two solutions are found and compared with the experimental data.

1 Introduction

The hadron spectrum is crucially shaped by the confinement property of QCD. It is often believed that in the sector of light mesons this property should lead to emergence of approximately linear Regge and radial trajectories with nearly universal slope. The hadron phenomenology seems to agree with this global feature of light meson spectrum, at least qualitatively [1–8]. The slope of angular and radial trajectories becomes a highly important quantity appearing from the non-perturbative QCD and giving rise to the scale of hadron masses in the light quark sector. Another important quantity in this picture represents the intercept which strongly depends on quantum numbers of a particular trajectory. The real meson spectrum reveals also deviations from the linear trajectories, sometimes quite noticeable. A pattern of these non-linear corrections remains obscure.

The problem of deciphering the general structure of light meson spectrum can be addressed by different methods. A fruitful approach closely related with QCD is the method of planar QCD sum rules (see, e.g., a short review in Ref. [9]). It is based on merging the ideas of classical SVZ sum rules [10]

and the large- N_c (often called planar) limit in QCD [11, 12]. Within the given method, the problem of description of non-linear corrections to the straight radial trajectories was studied in detail in Ref. [13]. In view of many phenomenological developments in the hadron spectroscopy in the last fourteen years we have found useful to check critically the conclusions made in Ref. [13] and try to use different assumptions in the proposed model. This constitutes the main purpose of the present work.

The paper is organized as follows. In Section 2, we formulate our model and derive the ensuing planar sum rules in the vector and scalar channels. Some insignificant errors noticed in Ref. [13] are corrected. The obtained equations are numerically solved in Section 3. The main new result here is finding the second solution which was missed in the original paper [13]. Our attempts to use alternative assumptions are briefly described in Section 4. We conclude in Section 5.

2 Sum rules

2.1 The two-point correlators

The QCD sum rules stem from the Operator Product Expansion (OPE) of two-point correlators of various quark currents in Euclidean space [10, 14] (see also the review [15]),

$$\Pi^J(Q^2) = \int d^4x e^{iQx} \langle \bar{q}\Gamma q(x)\bar{q}\Gamma q(0) \rangle, \quad (1)$$

where Q denotes the Euclidean momentum and we will consider the scalar (S), pseudoscalar (P), vector (V) and axial-vector (A) channels, i.e. $J = S, P, V, A$ corresponding to $\Gamma = i, \gamma_5, \gamma_\mu, \gamma_\mu\gamma_5$. The scalar part of vector and axial correlators is defined by

$$\Pi_{\mu\nu}^{V,A} = (-\delta_{\mu\nu}Q^2 + Q_\mu Q_\nu) \Pi^{V,A}(Q^2). \quad (2)$$

The OPE for these correlators at one-loop level and in the chiral limit reads [10, 14]

$$\Pi^V(Q^2) = \frac{1}{4\pi^2} \left(1 + \frac{\alpha_s}{\pi}\right) \ln \frac{\mu^2}{Q^2} + \frac{\alpha_s}{12\pi} \frac{\langle (G_{\mu\nu}^a)^2 \rangle}{Q^4} - \frac{28}{9} \pi \alpha_s \frac{\langle \bar{q}q \rangle^2}{Q^6}, \quad (3)$$

$$\Pi^A(Q^2) = \frac{1}{4\pi^2} \left(1 + \frac{\alpha_s}{\pi}\right) \ln \frac{\mu^2}{Q^2} + \frac{\alpha_s}{12\pi} \frac{\langle (G_{\mu\nu}^a)^2 \rangle}{Q^4} + \frac{44}{9} \pi \alpha_s \frac{\langle \bar{q}q \rangle^2}{Q^6}, \quad (4)$$

$$\Pi^S(Q^2) = -\frac{3}{8\pi^2} \left(1 + \frac{11\alpha_s}{3\pi}\right) Q^2 \ln \frac{\mu^2}{Q^2} + \frac{\alpha_s}{8\pi} \frac{\langle (G_{\mu\nu}^a)^2 \rangle}{Q^2} - \frac{22}{3} \pi \alpha_s \frac{\langle \bar{q}q \rangle^2}{Q^4}, \quad (5)$$

$$\Pi^P(Q^2) = -\frac{3}{8\pi^2} \left(1 + \frac{11\alpha_s}{3\pi}\right) Q^2 \ln \frac{\mu^2}{Q^2} + \frac{\alpha_s}{8\pi} \frac{\langle (G_{\mu\nu}^a)^2 \rangle}{Q^2} + \frac{14}{3} \pi \alpha_s \frac{\langle \bar{q}q \rangle^2}{Q^4}, \quad (6)$$

where $\langle \bar{q}q \rangle$ and $\langle (G_{\mu\nu}^a)^2 \rangle$ mean the quark and gluon condensate respectively and the further inverse in Q^2 terms are omitted. The numerical coefficients at the condensate contributions are given in the large- N_c limit of QCD [11, 12].

On the other hand, in the planar limit, the two-point correlators have the following resonance representation,

$$\Pi^J(Q^2) = \sum_{n=0}^{\infty} \frac{Z_J(n)}{Q^2 + m_J^2(n)}, \quad (7)$$

where n denotes the number of radial excitation.

The usual planar QCD sum rules are obtained after summing in n , decomposing the result in Q^{-2} , and matching to the corresponding OPE.

2.2 The vector and axial cases

Following the motivation of Ref. [13] (see also [16]) we consider the following form for the non-linear radial spectrum,

$$m_{V,A}^2(n) = M^2 + an + A_m^{V,A} e^{-B_m n}, \quad (8)$$

$$F_{V,A}^2(n) = a \left(C + A_F^{V,A} e^{-B_F n} \right). \quad (9)$$

Here $F_{V,A}^2(n) \equiv Z_{V,A}(n)/2$. The given ansatz consists from the linear part plus an exponentially decreasing correction (the physical spectrum corresponds to $B_m > 0$, $B_F > 0$). The form of this correction was dictated by the requirement to reproduce the analytical structure of OPE in the variable Q^2 [13].

To avoid the irrelevant infinite constants we will consider the first derivative in Q^2 . Introducing the notation

$$\bar{m}^2(n) = M^2 + an, \quad (10)$$

we obtain

$$\frac{d\Pi(Q^2)}{dQ^2} = -2 \sum_{n=0}^{\infty} \frac{a (C + A_F e^{-B_F n})}{(Q^2 + \bar{m}^2(n) + A_m e^{-B_m n})^2}. \quad (11)$$

This expression is not analytically summable and we need some approximation. Since the exponential contribution is presumably small except the

ground state $n = 0$, the further strategy is to keep only linear in exponential contribution terms for the excited states while the ground states are taken into account exactly. Below we display the resulting sum rules after matching to the OPE [13].

The sum rule at $1/Q^2$,

$$\frac{1}{8\pi^2} \left(1 + \frac{\alpha_s}{\pi}\right) = C. \quad (12)$$

The sum rules at $1/Q^4$,

$$a (C + A_F^V) - C \left(\frac{a}{2} + M^2\right) + A_F^V \Delta_F^{(1)} = 0, \quad (13)$$

$$a (C + A_F^A) - C \left(\frac{a}{2} + M^2\right) + A_F^A \Delta_F^{(1)} = -f_\pi^2. \quad (14)$$

The sum rules at $1/Q^6$,

$$\begin{aligned} -2a (C + A_m^V) (M^2 + A_m^V) + C \left(M^4 + M^2 a + \frac{a^2}{6}\right) \\ - 2CA_m^V \Delta_m^{(1)} - 2A_F^V \Delta_F^{(2)} = \frac{\alpha_s}{12\pi} \langle (G_{\mu\nu}^a)^2 \rangle, \end{aligned} \quad (15)$$

$$\begin{aligned} -2a (C + A_m^A) (M^2 + A_m^A) + C \left(M^4 + M^2 a + \frac{a^2}{6}\right) \\ - 2CA_m^A \Delta_m^{(1)} - 2A_F^A \Delta_F^{(2)} = \frac{\alpha_s}{12\pi} \langle (G_{\mu\nu}^a)^2 \rangle. \end{aligned} \quad (16)$$

The sum rule at $1/Q^8$ in $\Pi^V(Q^2) - \Pi^A(Q^2)$,

$$\begin{aligned} 3a (C + A_F^V) (M^2 + A_m^V)^2 - 3a (C + A_F^A) (M^2 + A_m^A)^2 \\ + 6C (A_m^V - A_m^A) \Delta_m^{(2)} + 3(A_F^V - A_F^A) \Delta_F^{(3)} = -12\pi\alpha_s \langle \bar{q}q \rangle^2. \end{aligned} \quad (17)$$

We introduced the following notations in the relations above,

$$\Delta_i^{(1)} = \frac{a}{e^{B_i} - 1}, \quad (18)$$

$$\Delta_i^{(2)} = \frac{a (-M^2 + (M^2 + a) e^{B_i})}{(e^{B_i} - 1)^2}, \quad (19)$$

$$\Delta_i^{(3)} = \frac{a \left(-a (a + 2M^2) + a e^{B_i} (2M^2 + 3a) + (M^2 + a)^2 (e^{B_i} - 1)^2\right)}{(e^{B_i} - 1)^3}. \quad (20)$$

2.3 The scalar and pseudoscalar cases

We define the scalar residues as

$$Z_{S,P}(n) = 2G_{S,P}^2(n)m_{S,P}^2(n). \quad (21)$$

For the π -meson, this definition makes sense if it belongs to the pseudoscalar radial trajectory. It looks more likely, however, that it does not belong to this trajectory because of its pseudogoldstone nature. In this case, we should use a current algebra relation $Z_\pi = 2\frac{\langle\bar{q}q\rangle^2}{f_\pi^2}$ [13]. We will consider the both cases and refer to them as π -in π -out correspondingly. Similarly to the vector channels, the scalar spectrum will be interpolated by the following ansatz [13],

$$m_{S,P}^2(n) = \bar{M}^2 + an + A_m^{S,P} e^{-B_m n}, \quad (22)$$

$$G_{S,P}^2(n) = a \left(\bar{C} + A_G^{S,P} e^{-B_G n} \right). \quad (23)$$

As was motivated in Ref. [13] the slope a and exponent B_m are considered as universal parameters determined mainly by pure gluodynamics.

Let us introduce the notation

$$\tilde{m}^2(n) = \bar{M}^2 + an, \quad (24)$$

and consider the cases π -out and π -in separately. To avoid the infinite contact terms, the second derivatives of the scalar correlators, $\frac{d^2\Pi(Q^2)}{(dQ^2)^2}$, will be analyzed. Using the procedure described above for the vector mesons we obtain the following set of sum rules for the case π -out [13].

The sum rule at $1/Q^2$,

$$\frac{3}{32\pi^2} \left(1 + \frac{11\alpha_s}{3\pi} \right) = \frac{\bar{C}}{2}. \quad (25)$$

The sum rules at $1/Q^6$,

$$a(\bar{C} + A_G^S)(\bar{M}^2 + A_m^S) - \frac{\bar{C}}{2} \left(\bar{M}^2(\bar{M}^2 + a) + \frac{a^2}{6} \right) + A_G^S \Delta_G^{(2)}(\bar{M}) + \frac{\mathbf{a}\bar{\mathbf{C}}\mathbf{A}_m^S}{\mathbf{e}^{\mathbf{B}_m} - \mathbf{1}} = \frac{\alpha_s}{16\pi} \langle (G_{\mu\nu}^a)^2 \rangle, \quad (26)$$

$$\frac{\langle\bar{q}q\rangle^2}{f_\pi^2} + a(\bar{C} + A_G^P)(\bar{M}^2 + A_m^P) - \frac{\bar{C}}{2} \left(\bar{M}^2(\bar{M}^2 + a) + \frac{a^2}{6} \right) + A_G^P \Delta_G^{(2)}(\bar{M}) + \frac{\mathbf{a}\bar{\mathbf{C}}\mathbf{A}_m^P}{\mathbf{e}^{\mathbf{B}_m} - \mathbf{1}} = \frac{\alpha_s}{16\pi} \langle (G_{\mu\nu}^a)^2 \rangle. \quad (27)$$

The sum rule at $1/Q^8$ in $\Pi^S(Q^2) - \Pi^P(Q^2)$,

$$-3a(\bar{C} + A_G^S)(\bar{M}^2 + A_m^S)^2 + 3a(\bar{C} + A_G^P)(\bar{M}^2 + A_m^P)^2 - 6\bar{C}(A_m^S - A_m^P)\Delta_m^{(2)}(\bar{M}) - 3(A_G^S - A_G^P)\Delta_G^{(3)}(\bar{M}) = -18\pi\alpha_s\langle\bar{q}q\rangle^2. \quad (28)$$

In these sum rules and in relations below, we write in bold face the contributions which were missed in Ref. [13].

The sum rules for the π -in case are the same but the terms containing the factor $(\bar{C} + A_G^P)$ are absent.

2.4 Chiral constants and electromagnetic pion mass difference

If the spectral parameters are obtained from the sum rules we can calculate the important constants L_{10} and L_8 of $SU(3)$ chiral perturbation theory [17] (the corresponding phenomenological values are $L_{10} = (-5.5 \pm 0.7) \cdot 10^{-3}$ and $L_8 = (0.8 \pm 0.3) \cdot 10^{-3}$) and the electromagnetic pion mass difference $\Delta m_\pi \equiv m_{\pi^+} - m_{\pi^0}$ (see, e.g., Ref. [18] for a short review), its experimental value is $\Delta m_\pi = 4.59$ MeV [19].

The corresponding chiral constants are defined by the relations

$$L_{10} = -\frac{1}{8} \frac{d}{dQ^2} (Q^2 (\Pi^V(Q^2) - \Pi^A(Q^2))) \Big|_{Q^2=0}, \quad (29)$$

$$L_8 = \frac{f_\pi^4}{32\langle\bar{q}q\rangle^2} \frac{d}{dQ^2} (Q^2 (\Pi^S(Q^2) - \Pi^P(Q^2))) \Big|_{Q^2=0}. \quad (30)$$

Substituting our ansatz and using our approximations we obtain

$$L_{10} = \frac{a}{4} \left(\frac{C + A_F^A}{M^2 + A_m^A} - \frac{C + A_F^V}{M^2 + A_m^V} + \sum_{n=1}^{\infty} \frac{\bar{m}^2(n) e^{-B_F n} (A_F^A - A_F^V) - C e^{-B_m n} (A_m^A - A_m^V)}{\bar{m}^4(n)} \right), \quad (31)$$

$$L_8 = \frac{f_\pi^4}{16\langle\bar{q}q\rangle^2} \left(\bar{C} + A_G^S + \frac{A_G^S - A_G^P}{e^{B_G} - 1} \right), \quad \text{case } \pi\text{-in}, \quad (32)$$

$$L_8 = \frac{f_\pi^4}{16\langle\bar{q}q\rangle^2} \frac{A_G^S - A_G^P}{1 - e^{-B_G}}, \quad \text{case } \pi\text{-out}. \quad (33)$$

The electromagnetic pion mass difference is given by

$$\Delta m_\pi = \frac{3\alpha}{16\pi m_\pi f_\pi^2} \int_0^\infty dQ^2 Q^2 (\Pi^A(Q^2) - \Pi^V(Q^2)). \quad (34)$$

Here α denotes the fine structure constant. This formula leads to the following expression [13],

$$\begin{aligned} \Delta m_\pi = \frac{3\alpha}{8\pi m_\pi f_\pi^2} & \left\{ (C + A_F^A)(M^2 + A_m^A) \ln(M^2 + A_m^A) \right. \\ & - (C + A_F^V)(M^2 + A_m^V) \ln(M^2 + A_m^V) + \sum_{n=1}^{\infty} \left[C \bar{m}^2(n) \ln \frac{m_A^2(n)}{m_V^2(n)} \right. \\ & \left. \left. + (C e^{-B_m n} (A_m^A - A_m^V) + \bar{m}^2(n) e^{-B_F n} (A_F^A - A_F^V)) \ln \bar{m}^2(n) \right] \right\}, \quad (35) \end{aligned}$$

where the dimensional quantities under the logarithms must be divided by arbitrary scale μ^2 . The result does not depend on μ^2 due to the imposed sum rules. The calculation of Ref. [13], however, was not carried out to its logical end: We keep only the linear in exponential corrections terms and this was not done for the first logarithm in the infinite sum. The correct calculation results in the final expression

$$\begin{aligned} \Delta m_\pi = \frac{3\alpha}{8\pi m_\pi f_\pi^2} & \left\{ (C + A_F^A)(M^2 + A_m^A) \ln(M^2 + A_m^A) \right. \\ & - (C + A_F^V)(M^2 + A_m^V) \ln(M^2 + A_m^V) + \frac{C(A_m^A - A_m^V)}{e^{B_m} - 1} \\ & \left. + \sum_{n=1}^{\infty} (C e^{-B_m n} (A_m^A - A_m^V) + \bar{m}^2(n) e^{-B_F n} (A_F^A - A_F^V)) \ln \bar{m}^2(n) \right\}. \quad (36) \end{aligned}$$

3 Numerical results

Having a set of sum rules and fixing some inputs one can calculate the mass spectrum in each channel. As inputs we take the masses of ground states $m_V(0)$, $m_A(0)$, $m_S(0)$, $m_P(0)$, and of first pseudoscalar excitation $m_P(1)$. Other inputs are taken as in Ref. [13]: $a = (1120 \text{ MeV})^2$, $\langle \bar{q}q \rangle = -(240 \text{ MeV})^3$, $\frac{\alpha_s}{\pi} \langle (G_{\mu\nu}^a)^2 \rangle = (360 \text{ MeV})^4$, $f_\pi = 103 \text{ MeV}$, $Z_\pi = 2 \frac{\langle \bar{q}q \rangle^2}{f_\pi^2}$, $\alpha_s = 0.3$. The units are: $m(n)$, $F(n)$, $G(n)$ — MeV; A_m — MeV²; A_F , A_G , $B_{F,G,m}$ — MeV⁰.

In comparing with phenomenological values we use the data from PDG [19] and try to neglect states with large admixture of s -quark and D -wave vector mesons.

3.1 Vector and axial-vector mesons

The mass spectrum ansatz (8)–(9) contains 9 parameters. We have 6 sum rules (12)–(17). The slope a is fixed from the phenomenology. Thus we need

2 additional constraints. These constraints will be the masses of ground states whose values are taken as in Ref. [13]: $m_V(0) = 770$ MeV, $m_A(0) = 1200$ MeV.

We found two numerical solutions for the system of equations (12)–(17) supplemented by 2 additional constraints, they are displayed in Tables 1-4 and Figs. 1,2. The first one is close to the solution found in Ref. [13] (where, e.g., $B_m = 0.97$ against our $B_m = 1.024$). A small difference is just due to a better precision of the present numerical calculation. To our surprise, there exists the second solution which was completely missed in Ref. [13]. The second solution corresponds to $B_m = 0.392$. It is seen that the experimental data are better described by the second solution.

It is worth noting that the electromagnetic pion mass difference Δm_π is very sensitive to the values of inputs $m_V(0)$ and $m_A(0)$. In fact, our choice above, which slightly differs from the corresponding central experimental values $m_V(0) = 775$ MeV and $m_A(0) = 1230$ MeV [19], was dictated by our wish to reproduce Δm_π close to its experimental value (with those central values Δm_π would be equal to 18 MeV in the first solution and 39 MeV in the second one). In this sense, Δm_π represents rather an input predicting a line on the parametric $(m_V(0), m_A(0))$ plane and a point on this line was chosen such that it provides the least mean square deviation from the experimental data.

Table 1: The parameters of solution in the vector case.

M, MeV	A_F^V	A_F^A	B_F	A_m^V , MeV ²	A_m^A , MeV ²	B_m	L_{10} , 10 ⁻³	Δm_π , MeV
925	0.001	-0.003	0.743	-(512) ²	(765) ²	1.024	-6.503	4.817
1215	0.003	0.	0.341	-(940) ²	-(191) ²	0.392	-6.638	5.436

Table 2: The mass spectrum of vector mesons (here and further in MeV).

B_m	$m_V(0)$	$m_V(1)$	$m_V(2)$	$m_V(3)$	$m_V(4)$
1.024	770	1420	1825	2146	2422
0.392	770	1461	1893	2229	2512
Exp.	775	1465 ± 25	1909 ± 17 ± 25	2254 ± 22	—

3.2 Scalar and pseudoscalar mesons

The mass spectrum ansatz (22)–(23) contains 9 parameters. We have 4 sum rules (25)–(28). By assumption, the slope a and exponent B_m are universal

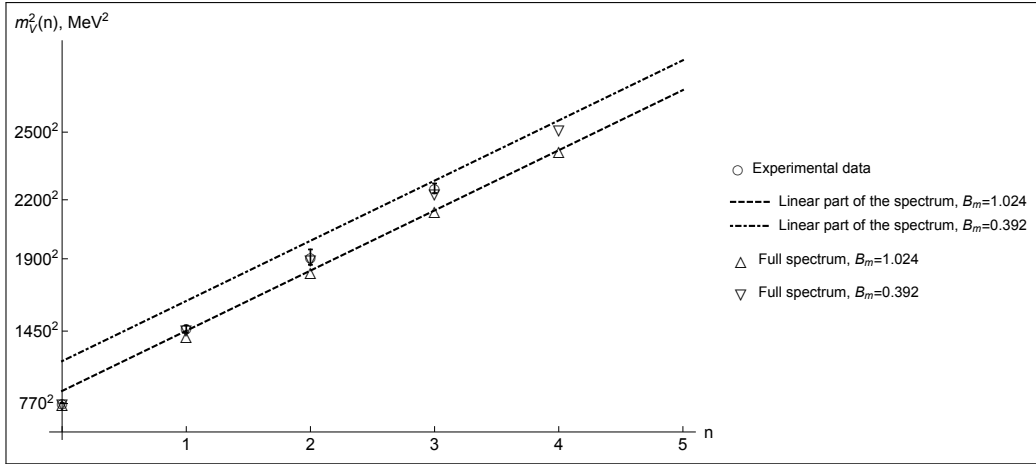


Figure 1: A graphical comparison of predicted and experimental vector spectrum.

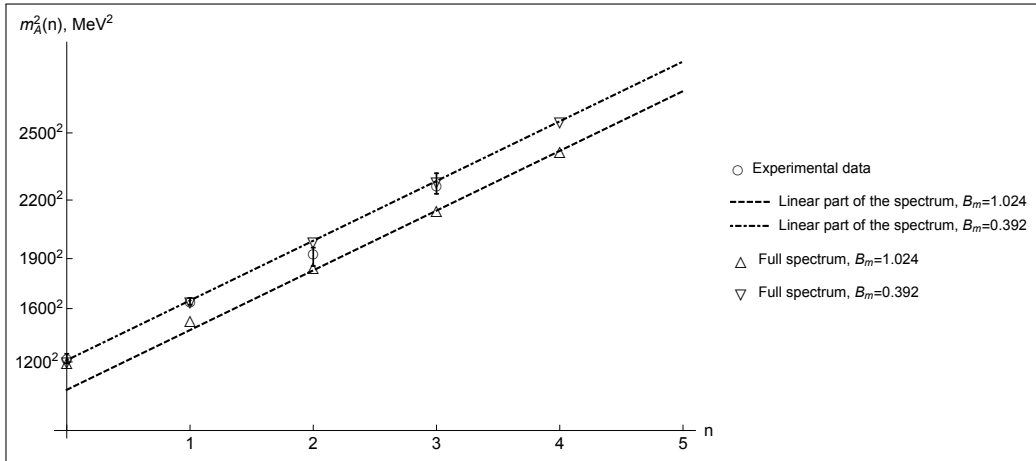


Figure 2: A graphical comparison of predicted and experimental axial spectrum.

Table 3: The mass spectrum of axial mesons.

B_m	$m_A(0)$	$m_A(1)$	$m_A(2)$	$m_A(3)$	$m_A(4)$
1.024	1200	1523	1855	2155	2425
0.392	1200	1645	1992	2287	2547
Exp.	1230 ± 40	1647 ± 22	1930^{+30}_{-70}	2270^{+55}_{-40}	—

Table 4: The predicted values of constants $F_{V,A}$.

B_m	$F_V(0)$	$F_V(1)$	$F_V(2)$	$F_V(3)$	$F_V(\infty)$	$F_A(0)$	$F_A(1)$	$F_A(2)$	$F_A(3)$	$F_A(\infty)$
1.024	138	135	133	133	132	116	125	129	130	132
0.392	144	141	138	136	132	133	133	133	132	132

parameters and we take them from the vector channel. Thus we need 3 additional constraints. Following Ref. [13] these constraints will be the masses of three states: $m_S(0) = 1000$ MeV, $m_P(0) = 0$, $m_P(1) = 1300$ MeV. Since the vector channel had two solutions with different values of exponent B_m , we will have two solutions in the scalar channels corresponding to two different fixations of B_m . In addition, we will consider separately the possibilities π -in and π -out. The calculated spectrum for all four variants is displayed and compared with the experimental data for f_0 and π mesons in Tables 5-12 and Plots 3-6. When there are two possible assignments for the predicted excited scalar mesons we show two lines for the experimental data in Tables 6 and 10.

Table 5: The parameters of solution in the scalar case π -in.

B_m	M , MeV	A_m^P , MeV ²	A_m^S , MeV ²	A_G^P	A_G^S	B_G	L_8 , 10 ⁻³
1.024	824	$-(824)^2$	$(566)^2$	0.004	-0.003	0.667	0.725
0.392	1159	$-(1159)^2$	$-(586)^2$	0.006	0.002	0.308	0.761

Table 6: The mass spectrum of scalar mesons in the π -in case.

B_m	$m_S(0)$	$m_S(1)$	$m_S(2)$	$m_S(3)$	$m_S(4)$
1.024	1000	1431	1797	2111	2388
0.392	1000	1538	1922	2236	2508
Exp.	990 ± 20	1200–1500	1723^{+6}_{-5}	2101 ± 7	2314 ± 25
		1504 ± 6	1992 ± 16	2189 ± 13	$2539 \pm 14^{+38}_{-14}$

The numerical effect of terms in Eqs. (25)–(28) displayed in bold face (missed in Ref. [13]) turned out to be small, far beyond the accuracy of the

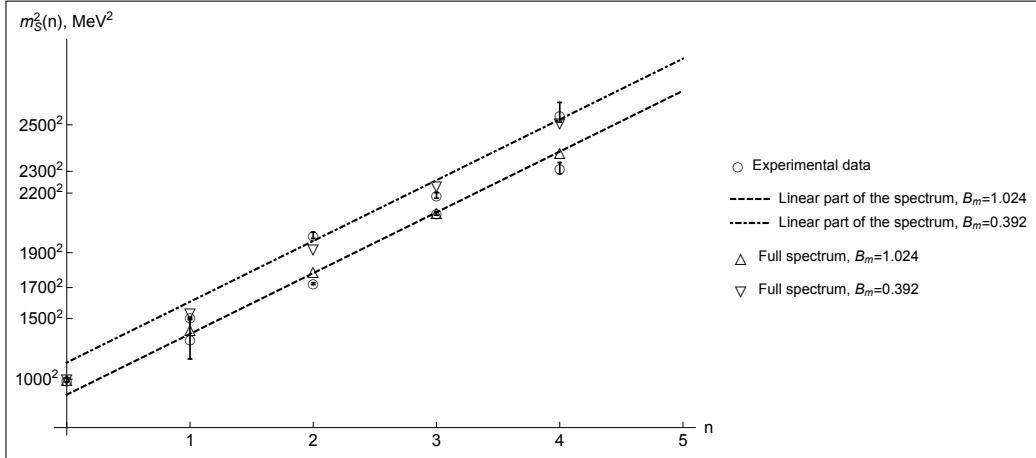


Figure 3: A graphical comparison of predicted and experimental scalar spectrum in the case π -in.

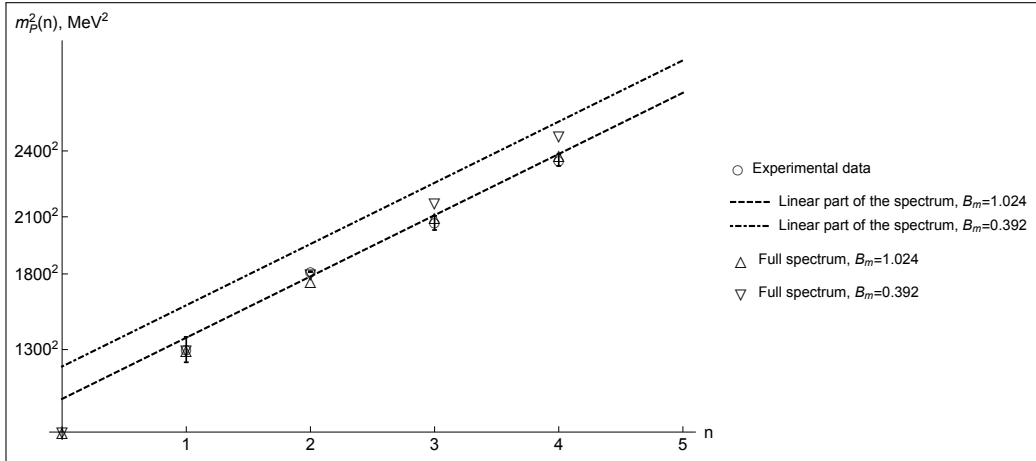


Figure 4: A graphical comparison of predicted and experimental pseudoscalar spectrum in the case π -in.

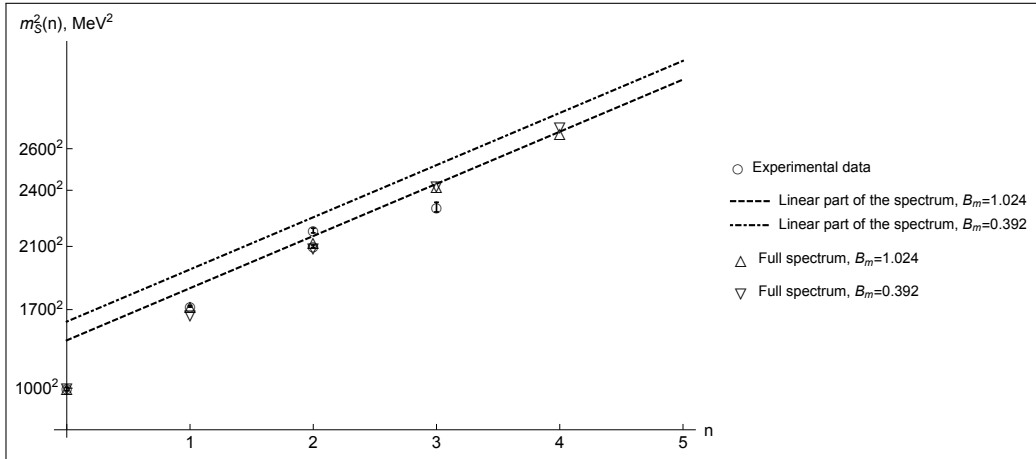


Figure 5: A graphical comparison of predicted and experimental scalar spectrum in the case π -out.

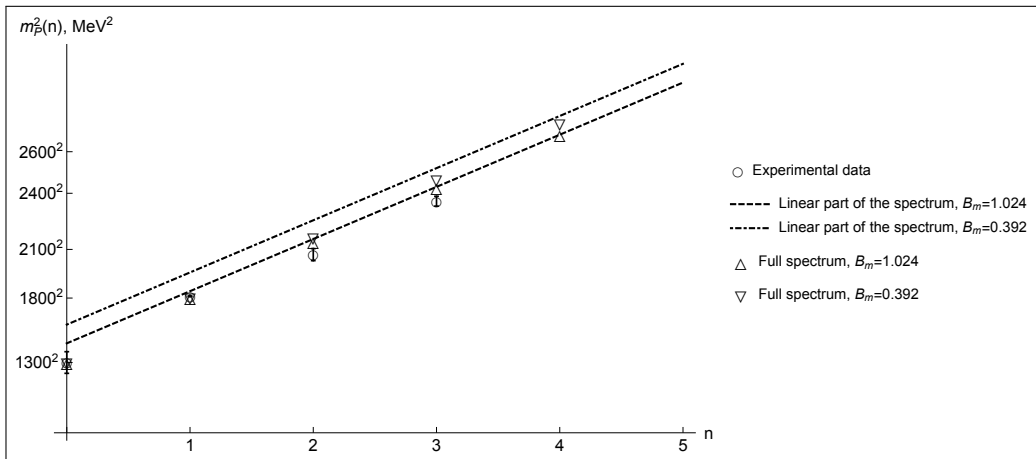


Figure 6: A graphical comparison of predicted and experimental pseudoscalar spectrum in the case π -out.

Table 7: The mass spectrum of pseudoscalar mesons in the π -in case.

B_m	$m_P(0)$	$m_P(1)$	$m_P(2)$	$m_P(3)$	$m_P(4)$
1.024	0	1300	1761	2100	2385
0.392	0	1300	1800	2166	2466
Exp.	—	1300 ± 100	1812 ± 12	2070 ± 35	2360 ± 25

Table 8: The predicted values of constants $G_{S,P}$ in the case π -in.

B_m	$G_P(0)$	$G_P(1)$	$G_P(2)$	$G_P(3)$	$G_P(\infty)$	$G_S(0)$	$G_S(1)$	$G_S(2)$	$G_S(3)$	$G_S(\infty)$
1.024	192	186	183	181	179	169	174	177	178	179
0.392	198	194	190	187	179	186	184	183	182	179

Table 9: The parameters of solution in the scalar case π -out.

B_m	M, MeV	A_m^P, MeV^2	A_m^S, MeV^2	A_G^P	A_G^S	B_G	$L_8, 10^{-3}$
1.024	1467	$-(679)^2$	$-(1073)^2$	0.008	0.025	1.181	1.147
0.392	1613	$-(955)^2$	$-(1266)^2$	0.007	0.012	0.408	0.747

Table 10: The mass spectrum of scalar mesons in the π -out case.

B_m	$m_S(0)$	$m_S(1)$	$m_S(2)$	$m_S(3)$	$m_S(4)$
1.024	1000	1730	2124	2421	2674
0.392	1000	1665	2093	2423	2699
Exp.	990 ± 20	1723_{-5}^{+6}	$\begin{matrix} 2189 \pm 13 \\ 2101 \pm 7 \end{matrix}$	2314 ± 25	—

Table 11: The mass spectrum of pseudoscalar mesons in the π -out case.

B_m	$m_P(0)$	$m_P(1)$	$m_P(2)$	$m_P(3)$	$m_P(4)$
1.024	1300	1800	2145	2428	2676
0.392	1300	1800	2167	2466	2726
Exp.	1300 ± 100	1812 ± 12	2070 ± 35	2360 ± 25	—

Table 12: The predicted values of constants $G_{S,P}$ in the case π -out.

B_m	$G_P(0)$	$G_P(1)$	$G_P(2)$	$G_P(3)$	$G_P(\infty)$	$G_S(0)$	$G_S(1)$	$G_S(2)$	$G_S(3)$	$G_S(\infty)$
1.024	205	188	182	180	179	252	205	187	182	179
0.392	202	195	190	186	179	218	206	197	192	179

large- N_c limit.

4 Further remarks

In the QCD sum rules, the quark and gluon condensates are external phenomenological parameters. It is interesting to check the impact of their values on our numerical solutions. Such a check was not done in Ref. [13]. We considered three radical possibilities: $\langle \bar{q}q \rangle = 0$, $\langle (G_{\mu\nu}^a)^2 \rangle = 0$, and $\langle \bar{q}q \rangle = \langle (G_{\mu\nu}^a)^2 \rangle = 0$. The caused shifts in numerical results turned out to be at the level of 1% or less, i.e. much less than the expected accuracy of our method based on the large- N_c limit.

The question may appear why we used the input $f_\pi = 103$ MeV which slightly differs from the corresponding phenomenological value $f_\pi = 93$ MeV? The reason is that for lower values of f_π our set of sum rules does not have any physical solutions. This feature was noticed in Ref. [13] and was confirmed by our present simulations.

The scalar resonance $f_0(500)$ is known to be very controversial (see, e.g. "Note on scalar mesons below 2 GeV" in [19] and recent review [20]). It is interesting thus to check whether our model is able to describe this state. We will proceed in the following way. The value of $m_S(0)$ will be decreased up to a point where the solutions cease to exist. The scalar and pseudoscalar mass spectrum for this minimal value of $m_S(0)$ is presented in Table 13. It

Table 13: The scalar and pseudoscalar mass spectrum for minimal value of $m_S(0)$.

	B_m	$m_S(0)$	$m_S(1)$	$m_S(2)$	$m_S(3)$	$m_S(4)$	$m_P(0)$	$m_P(1)$	$m_P(2)$	$m_P(3)$	$m_P(4)$
π -in	1.024	800	1386	1784	2107	2387	0	1300	1761	2100	2385
	0.392	700	1422	1861	2201	2487	0	1300	1800	2166	2466
π -out	1.024	1000	1730	2124	2421	2674	1300	1800	2145	2428	2676
	0.392	800	1591	2053	2400	2685	1300	1800	2167	2466	2726

is seen that the second solution permits a lower value of $m_S(0)$. In any case there is no solution near 500 MeV.

Our ansatz for non-linear corrections distorts the linear trajectories in one direction. This may look unnatural because one might expect that the physical masses are scattered uniformly near both sides of straight radial Regge trajectory. The given feature may be modeled by adding extra factor $(-1)^n$ in front of the exponential correction which makes this correction sign-alternating,

$$m_{V,A}^2(n) = M^2 + an + (-1)^n A_m^{V,A} e^{-B_m n}. \quad (37)$$

This ansatz leads to the following sum rules in the vector sector (the changes caused by the sign-alternating modification of ansatz are shown in bold face):

The sum rule at $1/Q^2$,

$$\frac{1}{8\pi^2} \left(1 + \frac{\alpha_s}{\pi}\right) = C.$$

The sum rules at $1/Q^4$,

$$a (C + A_F^V) - C \left(\frac{a}{2} + M^2\right) + A_F^V \Delta_F^{(1)} = 0, \quad (38)$$

$$a (C + A_F^A) - C \left(\frac{a}{2} + M^2\right) + A_F^A \Delta_F^{(1)} = -f_\pi^2. \quad (39)$$

The sum rules at $1/Q^6$,

$$\begin{aligned} -2a (C + A_F^V) (M^2 + A_m^V) + C \left(M^4 + M^2 a + \frac{a^2}{6}\right) + \frac{2\mathbf{C}\mathbf{A}_m^V}{\mathbf{e}^{\mathbf{B}_m} + 1} \\ - 2A_F^V \Delta_F^{(2)} = \frac{\alpha_s}{12\pi} \langle (G_{\mu\nu}^a)^2 \rangle, \end{aligned} \quad (40)$$

$$\begin{aligned} -2a (C + A_F^A) (M^2 + A_m^A) + C \left(M^4 + M^2 a + \frac{a^2}{6}\right) + \frac{2\mathbf{C}\mathbf{A}_m^A}{\mathbf{e}^{\mathbf{B}_m} + 1} \\ - 2A_F^A \Delta_F^{(2)} = \frac{\alpha_s}{12\pi} \langle (G_{\mu\nu}^a)^2 \rangle. \end{aligned} \quad (41)$$

The sum rule at $1/Q^8$ in $\Pi^V(Q^2) - \Pi^A(Q^2)$,

$$\begin{aligned} 3a (C + A_F^V) (M^2 + A_m^V)^2 - 3a (C + A_F^A) (M^2 + A_m^A)^2 + \\ \mathbf{6C} (\mathbf{A}_m^A - \mathbf{A}_m^V) \left(\frac{\mathbf{M}^2}{\mathbf{e}^{\mathbf{B}_m} + 1} + \frac{\mathbf{a}\mathbf{e}^{\mathbf{B}_m}}{(\mathbf{e}^{\mathbf{B}_m} + 1)^2} \right) \\ + 3(A_F^V - A_F^A) \Delta_F^{(3)} = -12\pi\alpha_s \langle \bar{q}q \rangle^2. \end{aligned} \quad (42)$$

Our numerical simulations, however, did not result in any physically reasonable solution.

5 Conclusions

The spectroscopic models based on the planar QCD sum rules remain a viable non-perturbative approach to the spectroscopy of light mesons.

In the given work, we critically reassessed the analysis of radial Regge trajectories with non-linear corrections performed in Ref. [13] for the vector, axial, scalar, and pseudoscalar trajectories. Some errors in the expressions for the sum rules in the scalar channel and for the electromagnetic pion mass

difference were found. Their influence on the numerical solutions, however, is negligible. The main finding was the discovery of the second solution in the considered planar sum rules. The global description of the experimental data for vector and axial mesons happens to be better in the case of the second solution. In the scalar and pseudoscalar sectors, the quality of description seems to be comparable for both solutions.

We confirmed the conclusion of Ref. [13] that the lowest scalar meson cannot be made significantly lighter 1 GeV within the considered approach. We checked the dependence of numerical results on the values of vacuum condensates in the OPE and found it negligible within the accuracy of the given large- N_c method. The planar sum rules for a sign-alternating exponential correction to the radial trajectories were derived and analyzed numerically. We could not detect any physically acceptable numerical solution for this ansatz. We observed an extremely strong sensitivity of electromagnetic pion mass difference to the masses of lowest vector and axial mesons. The fact that the physical value of this difference is achieved with input masses very close to their central experimental values seems to represent a nontrivial and interesting result.

It could be interesting to extend the present analysis to sectors with other quantum numbers and to light mesons with open and hidden strangeness.

References

- [1] A. V. Anisovich, V. V. Anisovich and A. V. Sarantsev, Phys. Rev. D **62**, 051502(R) (2000).
- [2] D. V. Bugg, Phys. Rep. **397**, 257 (2004).
- [3] E. Klempt and A. Zaitsev, Phys. Rep. **454**, 1 (2007).
- [4] M. Shifman and A. Vainshtein, Phys. Rev. D **77**, 034002 (2008).
- [5] S. S. Afonin, Eur. Phys. J. A **29**, 327 (2006).
- [6] S. S. Afonin, Mod. Phys. Lett. A **22**, 1359 (2007).
- [7] S. S. Afonin, Phys. Rev. C **76**, 015202 (2007).
- [8] P. Masjuan, E. Ruiz Arriola and W. Broniowski, Phys. Rev. D **85**, 094006 (2012).
- [9] S. S. Afonin and T. D. Solomko, Eur. Phys. J. C **76**, 678 (2016).

- [10] M. A. Shifman, A. I. Vainshtein and V. I. Zakharov, Nucl. Phys. B **147**, 385, 448 (1979).
- [11] G. 't Hooft, Nucl. Phys. B **72**, 461 (1974).
- [12] E. Witten, Nucl. Phys. B **160**, 57 (1979).
- [13] S. S. Afonin, A. A. Andrianov, V. A. Andrianov and D. Espriu, JHEP **0404**, 039 (2004).
- [14] L.J. Reinders, H. Rubinstein, S. Yazaki, Phys. Rept. **127**, 1 (1985).
- [15] P. Colangelo and A. Khodjamirian, hep-ph/0010175.
- [16] S. S. Afonin, Nucl. Phys. B **779**, 13 (2007).
- [17] J. Gasser and H. Leutwyler, Nucl. Phys. B **250**, 465 (1985).
- [18] V. A. Andrianov and S. S. Afonin, Phys. Atom. Nucl. **65**, 1862 (2002).
- [19] C. Patrignani *et al.* (Particle Data Group), Chin. Phys. C **40**, 100001 (2016).
- [20] J. R. Pelaez, Phys. Rept. **658**, 1 (2016).